Electronic Supplementary Information

Winolides A–C, bioactive sesquiterpene lactones with unusual 5,6-secoeudesmane frameworks from *Inula wissmanniana*†

Xiang-Rong Cheng,‡[ab] Wen-Hao Shao,‡[c] Shou-De Zhang,‡[a] Guo-Wei Wang,[a] Lei Shan,[c] Yun-Heng Shen,[c] Qing-Yan Sun,*[c] Hui-Zi Jin[a] and Wei-Dong Zhang*[ac]

[a] *School of Pharmacy, Shanghai Jiao Tong University, Shanghai 200240, P. R. China. E-mail: wdzhangy@hotmail.com; Tel: +86-21-34205989; Fax: +86-21-34205989*

[b] *School of Food Science and Technology, Jiangnan University, Wuxi 214122, Jiangsu Province, P. R. China*

[c] *School of Pharmacy, Second Military Medical University, Shanghai 200433, P. R. China. E-mail: sqy_2000@163.com*

* Corresponding authors. Tel./Fax: +86-021-34205989.

E-mail: sqy_2000@163.com (Q.-Y. Sun); wdzhangy@hotmail.com (W.-D. Zhang).

1 General experimental procedures

Optical rotations were measured on a Jasco P-2000 polarimeter. UV spectra were measured on a Shimadzu UV-2550 spectrophotometer. CD experiments were operated on a JASCO J-815 CD spectrometer. IR spectra were performed on Bruker FTIR Vector 22 spectrometer. NMR experiments were recorded on a Bruker Avance Ⅲ spectrometer (for ^{1}H NMR at 400 MHz and ^{13}C NMR at 100 MHz) using TMS as an internal standard. ESIMS were measured on an Agilent 1100 series mass spectrometer. HREIMS were acquired using a MAT-212 magnetic sector mass spectrometer. Column chromatographic separations were carried out by using silica gel (100-200 mesh and 200-300 mesh, Qingdao Haiyang Chemical Group Corporation, Qingdao, China), MCI gel CHP-20P (75-150 μM; Mitsubishi Chemical Industries Co. Ltd.), Sephadex LH-20 (Pharmacia Biotech AB, Uppsala, Sweden) as packing materials. Preparative HPLC was conducted on a Shimadzu LC-6AD series equipped with an SPD-20 spectrophotometer using Shimadzu PRC-ODS EV0233 column at flow rate 8 mL/min.

2 Isolation procedure of compounds 1–3

The whole plants of *I. wissmanniana* were collected from Pingbian county, Yunnan province, PR China, in August 2010, and identified by Prof. Han-Ming Zhang (Department of Pharmacognosy, Second Military Medical University). A voucher specimen (No. DJ 20100801) has been deposited at School of Pharmacy, Shanghai Jiao Tong University, Shanghai, PR China.

The air-dried whole plants of *I. wissmanniana* (10.0 kg) were chopped and percolated with 95% EtOH four times (30 L, 24 h, 12 h, 12 h, 12 h) at room temperature to give 631.4 g of crude extract, which was suspended in water and then extracted with petroleum ether (PE, 60–90 ºC) to remove the fatty components. The residual crude extract was further partitioned with CH_2Cl_2 to give a CH_2Cl_2-soluble fraction (179.6 g). A part of the CH_2Cl_2-soluble fraction (119.2 g) was subjected to silica gel (100–200 mesh) column chromatography (10 × 100 cm) eluted successively with CH_2Cl_2/MeOH gradient (100: 0 to 0: 1, v/v) to give eight fractions (A–H). Fraction A (17.0 g) was applied to a silica gel column (200–300 mesh, 6 × 70 cm) eluted with PE/ethyl acetate (EtOAc) (20: 1, v/v) to afford subfractions A1–A6. Subfraction A3 was further purified by preparative HPLC (70 % MeOH as eluant) to yield compounds **3** (t_R 28.8 min, 1.5 mg) and **2** (t_R 30.9 min, 2.5 mg). Subfraction A4 was further purified by preparative HPLC (70 % MeOH as eluant) to yield compound **1** (t_R 32.5 min, 10.0 mg). The purity of **1**–**3** (> 98.0%) was analyzed by HPLC.

3 Optical rotation and ECD calculations of 1

3.1 Conformational analysis

Conformational searching was carried out using molecular mechanics (MM) methods with the MMFF94 force field in Maestro7.5. The obtained conformations were re-optimized using *ab initio* DFT at the B3LYP/6-31G** level to give stable conformers of the enantiomers (*S*-**1**, *R*-**1**), three of which were further determined as mainly populated conformers for each enantiomer (*S*-**1a**–*S*-**1c**, *R*-**1a**–*R*-**1c**, **Tables S1 and S2**). Frequencies of stable conformations were calculated and led to the relative free energies, which in turn allow the room temperature equilibrium populations to be calculated according to Maxwell-Boltzmann distribution law.

$$\frac{N_i^*}{N} = \frac{g_i e^{-\varepsilon_i / k_B T}}{\sum g_i e^{-\varepsilon_i / k_B T}}$$

Table S1 Important thermodynamic parameters and conformational analysis of *S*-**1**

Conformer	ΔE^a	ΔE^b	ΔE^c	ΔG^d	$P(\%)^e$	$P(\%)^f$	$P(\%)^g$	$P(\%)^h$
S-**1a**	0.00	0.00	0.00	0.00	54.75	54.01	54.34	54.32
S-**1b**	0.37	0.38	0.37	0.32	29.54	28.33	29.00	31.49
S-**1c**	0.86	0.81	0.83	0.91	12.79	13.76	13.28	11.60
S-**1d**	2.20	2.03	2.10	2.45	1.34	1.75	1.56	0.86
S-**1e**	2.31	2.14	2.23	2.18	1.11	1.45	1.25	1.38
S-**1f**	2.95	2.70	2.83	3.16	0.38	0.57	0.46	0.26
S-**1g**	4.37	4.21	4.29	4.47	0.03	0.04	0.04	0.03
S-**1h**	3.95	3.80	3.93	4.09	0.07	0.09	0.07	0.05

[a-c,] Relative energies at B3LYP/6-31G(d) level in the MeOH, $CHCl_3$, and CH_2Cl_2, respectively (kcal/mol). [d] Relative Gibbs free energy at B3LYP/6-31G(d) level in the gas phase (kcal/mol). [e-g] Conformational distribution calculated by corresponding ΔE, T = 298 K. [h] Conformational distribution calculated by the Gibbs free energy at B3LYP/6-31G(d) level in the gas phase T = 298 K.

Table S2 Important thermodynamic parameters and conformational analysis of *R*-**1**

Conformer	ΔE^a	ΔE^b	ΔE^c	ΔG^d	$P(\%)^e$	$P(\%)^f$	$P(\%)^g$	$P(\%)^h$
R-**1a**	0.00	0.00	0.00	0.00	52.59	53.74	54.16	54.38
R-**1b**	0.35	0.38	0.37	0.32	29.22	28.53	29.16	31.45
R-**1c**	0.76	0.81	0.83	0.92	14.50	13.80	13.26	11.58
R-**1d**	2.18	2.03	2.10	2.45	1.33	1.76	1.58	0.86
R-**1e**	2.05	2.13	2.22	2.18	1.66	1.47	1.27	1.37
R-**1f**	2.65	2.69	2.82	3.16	0.60	0.57	0.46	0.26
R-**1g**	4.40	4.20	4.28	4.47	0.03	0.04	0.04	0.03
R-**1h**	3.90	3.80	3.92	4.09	0.07	0.09	0.07	0.05

[a-c,] Relative energies at B3LYP/6-31G(d) level in the MeOH, $CHCl_3$, and CH_2Cl_2, respectively (kcal/mol). [d] Relative Gibbs free energy at B3LYP/6-31G(d) level in the gas phase (kcal/mol). [e-g] Conformational distribution calculated by corresponding ΔE, T = 298 K. [h] Conformational distribution calculated by the Gibbs free energy at B3LYP/6-31G* level in the gas phase T = 298 K.

3.2 Optical rotation values calculation

The optical rotation values of *S*-**1a**–*S*-**1c** and *R*-**1a**–*R*-**1c** were calculated at the B3LYP-SCRF/6-31G(d)//B3LYP/6-311++G(2d, p) level with the PCM model in CH_2Cl_2 solution, which were further weighted by Boltzmann population to give the rotation values of *S*-**1** and *R*-**1** (**Table S3**). The calculated optical rotation values of *S*-**1** and *R*-**1** were further compared with the experimental values of **1**, **3**, *S*-**8**, and *R*-**8** (**Table S3**).

Table S3 Calculated optical rotation values of **1** and experimental values of **1**, **3**, and **8**

Conformers	Calculated $[\alpha]_D$[a]				Exp. $[\alpha]_D$
	a	**b**	**c**	Weighted[b]	
S-**1**	+ 93.5	– 347.69	– 214.08	– 78.2	/
R-**1**	– 93.4	+ 347.69	+ 214.07	+ 78.2	/
1			/		– 91.2[c]
3			/		– 16.6[d]
S-**8**			/		– 37.9[c]
R-**8**			/		+ 28.3[c]

[a] The optical rotation value were calculated at the B3LYP-SCRF/6-31G(d)//B3LYP/6-311++G(2d, p) level with the PCM model in CH_2Cl_2; [b] Weighted by the Boltzmann population (*g* of Table S1 and Table S2); [c] CH_2Cl_2, *c* 0.1; [d] CH_2Cl_2, *c* 0.05.

3.3 Original ECD data calculations

Excitation energy (in nm) and rotatory strength *R* (velocity form R^{vel} and length form R^{len} in 10^{-40} erg-esu-cm/Gauss) between different states were calculated using TDDFT method at B3LYP/6-31G*//B3LYP/6-31G* level with the PCM model in methanol solution. All the calculations were performed with the Gaussian03 program.

Table S4 Key transitions, oscillator strengths, and rotatory strengths in the ECD spectra of conformers of *S*-**1b** at B3LYP/6-31G* Level in the MeOH

Species	**Excited State**	***ΔE*[a] (eV)**	***λ*[b]*(nm)***	***f*[c]**	***R*^vel [d]**	***R*^len [e]**
S-**1b**	62 -> 63	4.4798	276.76	0.0065	-7.8425	-8.3107
	61 -> 63	4.5993	269.57	0.0010	0.8829	0.7874
	59 -> 63	4.8780	254.17	0.0011	3.6076	4.2885
	61 -> 64	5.2825	234.71	0.0020	-0.5517	-0.5074
	60 -> 63	5.8288	212.71	0.1999	-94.5520	-101.5657
	62 -> 64	5.8914	210.45	0.0644	27.3154	27.3091

[a] Excitation energy. [b] Wavelength. [c] Oscillator strength. [d] Rotatory strength in velocity form (10^{-40}cgs.) [e] Rotatory strength in length form (10^{-40}cgs.).

3.4 ECD simulation

The ECD spectra were then simulated by overlapping Gaussian functions for each transition according to

$$\Delta\varepsilon(E) = \frac{1}{2.297\times10^{-39}} \times \frac{1}{\sqrt{2\pi\sigma}} \sum_{i}^{A} \Delta E_i R_i e^{-[(E-E_i)/(2\sigma)]^2}$$

where σ is the width of the band at 1/e height, and *ΔEi* and *Ri* are the excitation energies and rotatory strengths for transition *i*, respectively. σ = 0.20 eV and R^{vel} have been used in this work. Conformational analysis has been carried out and theoretically weighted ECD spectra have been simulated at different levels mentioned above (**Fig. S1** and **S2**).

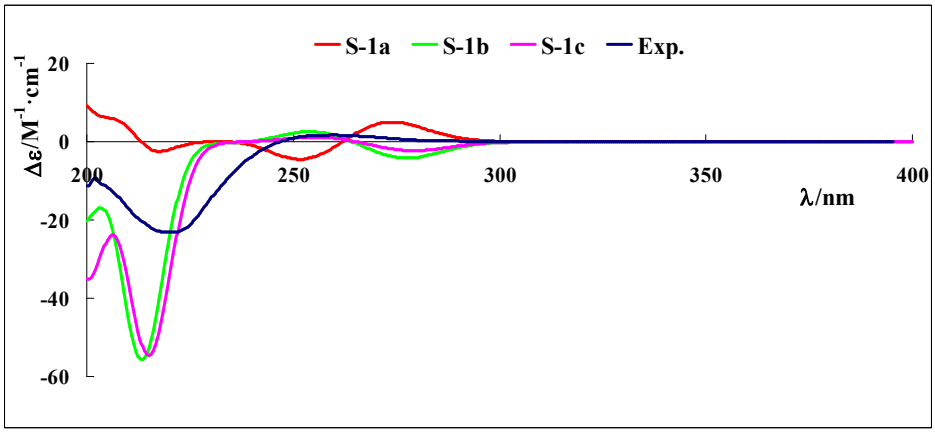

Fig. S1 The experimental CD spectrum of **1** and calculated ECD Spectra of *S*-**1a**–*S*-**1c** at B3LYP-SCRF/6-31G*//B3LYP/6-31G* level with the COSMO model in methanol solution

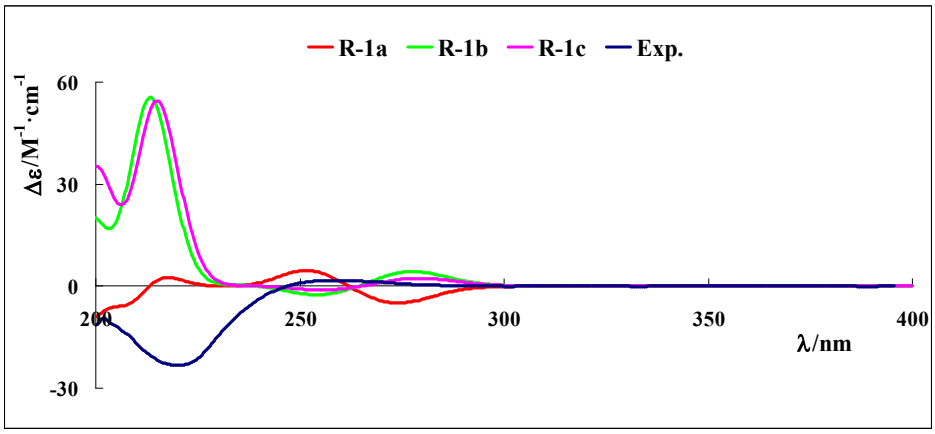

Fig. S2 The experimental CD spectrum of **1** and calculated ECD Spectra of *R*-**1a**–*R*-**1c** at B3LYP-SCRF/6-31G*//B3LYP/6-31G* level with the COSMO model in methanol solution

4 Asymmetric total synthesis of 8

(*Z*)-4-Hydroxybut-2-en-1-yl propiolate (4)

DCC (2.79 g, 13.5 mmol) and DMAP (0.12 g, 0.09 mmol) in dichloromethane (30 mL) was added dropwise over 20 min to a solution of (*Z*)-but-2-ene-1,4-diol (1.05 g，12.0 mmol) and propiolic acid (0.93 g, 13.2 mmol) in dichloromethane (20 mL) at –30 °C. The reaction mixture was allowed to stir at rt for 12h. Then quenched with sat. aq NH_4Cl (30 mL). The aq. layer was extracted with dichloromethane (3 × 15 mL) and the combined organic extracts dried (Na_2SO_4), concentrated under reduced pressure and purified by column chromatography to give **4** (1.41 g, 76%) as yellow oil.

^{1}H NMR (500 MHz, $CDCl_3$): δ 5.82 (dt, J = 11.6, 6.4 Hz, 1H), 5.59 (dt, J = 11.2, 7.0 Hz, 1H), 4.73 (d, J = 7.0 Hz, 2H), 4.20 (d, J = 6.3 Hz, 2H), 2.83 (s, 1H); ^{13}C NMR (125 MHz, $CDCl_3$): δ 152.73, 134.57, 124.26, 75.28, 74.55, 61.85, 58.59; HR-ESI-MS calcd for $C_7H_9O_3$ $[M + H]^+$ 141.1366, found 141.1362.

2-(4-Methylene-5-oxotetrahydrofuran-3-yl)acetaldehyde (5)

$[Rh(cod)Cl]_2$ (50.2 mg, 0.102 mol) and $AgSbF_6$ (70.0 mg, 0.204 mol) were added to a three-necked vial with a stir bar and rubber bung. The air was removed by refilling with argon (three times). Acetone (10 ml) was added to the mixture by a syringe. After stirring at rt for 20 min, the yellow suspension was

filtered under argon into a flask containing (*R*/*S*)-BINAP (127 mg, 0.204 mol). The resulting solution was stirred for 20 min, then added to a solution of **4** (1.14 g, 8.14 mmol) in 1,2-dichlorethane (20 mL) at rt. The reaction mixture was stirred for 21 h at rt, then concentrated under reduced pressure and purified by column chromatography to give **5** (0.67 g, 59%) as yellow oil. The purified reaction products were further analyzed by HPLC equipped with a CHIRALCEL OD-RH column (Daicel Chiral Technologies Co., Ltd., China) to afford peak area ratios of enantiomers (**Fig. S3** and **S4**). The ee values for enantiomers **5** were calculated according to the following formula: ee% = (a-b)/(a+b).

^{1}H NMR (600 MHz, $CDCl_3$): δ 9.82 (s, 1H), 6.31 (d, J = 2.9 Hz, 1H), 5.65 (d, J = 2.6 Hz, 1H), 4.65 (dd, J = 9.3, 8.6 Hz, 1H), 3.92 (dd, J = 9.4, 5.9 Hz, 1H), 3.58 (ddt, J = 11.2, 5.7, 3.0 Hz, 1H), 2.99 (dd, J = 19.0, 5.1 Hz, 1H), 2.79 (dd, J = 19.0, 8.7 Hz, 1H); ^{13}C NMR (150 MHz, $CDCl_3$): δ 199.15, 170.23, 137.45, 123.00, 77.16, 71.14, 48.33, 33.18; HR-ESI-MS calcd for $C_7H_9O_3$ $[M + H]^+$ 141.1366, found 141.1370; *S*-**5**: [α]20 D – 47.3 (*c* 0.1, CH_2Cl_2), ee% = 89.78%; *R*-**5**: [α]20 D + 75.2 (*c* 0.1, CH_2Cl_2), ee% = 92.22%.

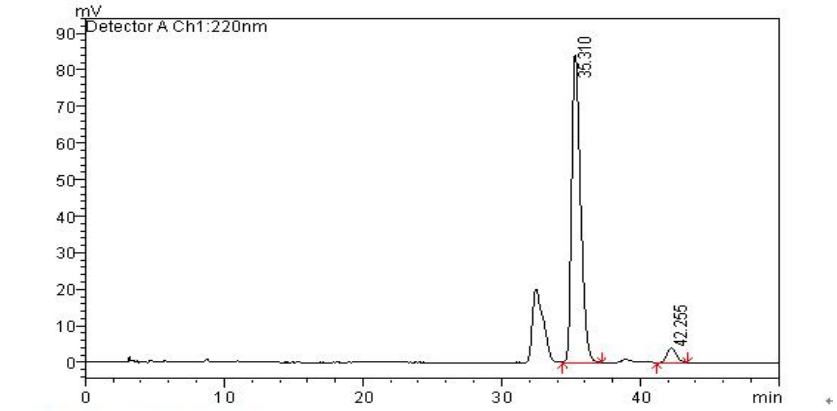

<Column Performance Report>

Peak No.	Time	Area	Area %	Plate number	Tailing	Resolution
1	35.310	3761224	94.8923	14336.469	1.402	--
2	42.255	202452	5.1077	16774.287	1.109	5.591

Fig. S3 The trace of *S*-**5** through the chiral HPLC column.

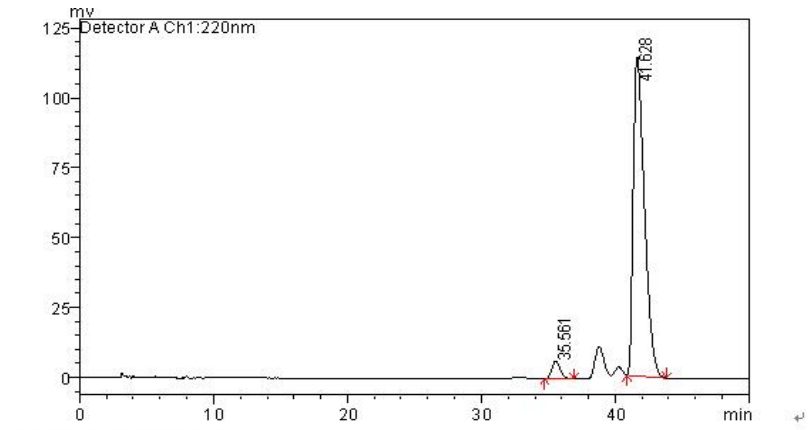

<Column Performance Report>

Peak No.	Time	Area	Area %	Plate number	Tailing	Resolution
1	35.561	267833	3.8913	16675.182	1.157	--
2	41.628	6615080	96.1087	11611.158	1.755	4.585

Fig. S4 The trace of *R*-**5** through the chiral HPLC column.

4-(2-Hydroxyethyl)-3-methylenedihydrofuran-2(3H)-one (6)

BH_3·THF (0.31 mL, 1 M in THF, 0.31 mmol) was added to a solution of aldehydes **5** (39 mg, 0.28 mmol) in THF (1 mL) at 0 °C. The reaction mixture was stirred 10min at rt, then quenched with sat. aq NH_4Cl (5 mL). The aq layer was extracted with EtOAc (3 × 5 mL) and the combined organic extracts dried (Na_2SO_4), concentrated under reduced pressure and purified by column chromatography to give **6** (0.26 g, 65%) as yellow oil.

^{1}H NMR (500 MHz, $CDCl_3$): δ 6.27 (d, J = 2.8 Hz, 1H), 5.63 (d, J = 2.5 Hz, 1H), 4.55–4.51 (m, 1H), 4.07 (dd, J = 9.1, 5.9 Hz, 1H), 3.79–3.72 (m, 2H), 3.29–3.23 (m, 1H), 1.94 (ddd, J = 14.0, 11.4, 5.6 Hz, 1H), 1.81–1.73 (m, 1H); ^{13}C NMR (125 MHz, $CDCl_3$): δ 171.05, 138.35, 122.23, 71.69, 60.03, 36.53, 36.13; HR-ESI-MS calcd for $C_7H_{11}O_3$ $[M + H]^+$ 143.1525, found 143.1520; *S*-**6**: [α]20 D – 22.1 (*c* 0.1, CH_2Cl_2); *R*-**6**: [α]20 D + 40.3 (*c* 0.1, CH_2Cl_2).

4-(2-bromoethyl)-3-methylenedihydrofuran-2(3H)-one (7)

PPh_3 (157 mg, 0.6 mmol） and CBr_4 (199 mg, 0.6 mmol) was added to a solution of **6** (71 mg, 0.5 mmol) in CH_2Cl_2 (10 ml). The reaction mixture was stirred for 2 h at rt, then concentrated under reduced pressure and purified by column chromatography to give **7** (79 mg, 77%) as yellow oil. The analysis of ^{1}H NMR spectrum (figure S32) suggested that there were side reactions during the bromination of **6**, although the reaction products shared the same R_f value and HR-ESI-MS data. The side products might be isomers of **7**.

^{1}H NMR (500 MHz, $CDCl_3$): δ 6.34 (d, J = 2.4 Hz, 1H), 5.70 (d, J = 2.2 Hz, 1H), 4.52 (dd, J = 9.0, 8.0 Hz, 1H), 4.04 (dd, J = 9.2, 4.7 Hz, 1H), 3.45 (t, J = 6.4 Hz, 2H), 3.36 (ddd, J = 7.3, 5.1, 2.6 Hz, 1H), 2.23–2.17 (m, 1H), 2.13–2.06 (m, 1H); ^{13}C NMR (125 MHz, $CDCl_3$): δ 170.26, 137.13, 123.07, 70.65, 37.51, 36.26, 29.73; HR-ESI-MS calcd for $C_7H_9O_2Br$ $[M]^+$ 205.0491, found 205.0459; IR (KBr) ν_{max} 2945, 1726, 1660, 1523, 1457, 1298, 1265, 1085, 877, 675 cm^{-1}; *S*-**7**: [α]20 D – 11.5 (*c* 0.05, CH_2Cl_2); *R*-**8**: [α]20 D + 16.8 (*c* 0.05, CH_2Cl_2).

3-methylene-4-phenethyldihydrofuran-2(3H)-one (8)

$PdBr_2$ (10.6 mg, 0.04 mmol) and $[HP(t\text{-}Bu)_2Me]BF_4$ (24.8 mg, 0.10 mmol) were placed in a vial equipped with a stir bar. The air was removed by refilling with argon (three times). THF (2.5 ml) and TBAF (0.1 ml, 1 M in THF) were added, the resulting mixture was stirred for 30 min at rt. This solution was added $(MeO)_3SiPh$ (224 μL, 1.2 mmol), TBAF (2 ml), and alkyl bromides **7** (205 mg, 1.0 mmol). The reaction mixture was stirred at rt for 14 h, then filtered through a pad of silica gel (washed with 50 ml EtOAc), concentrated, and purified by column chromatography to give **8** (108 mg, 53%) as yellow oil.

^{1}H NMR (500 MHz, $CDCl_3$): δ 7.31 (t, J = 7.4 Hz, 2H), 7.23 (t, J = 7.3 Hz, 1H), 7.18 (d, J = 7.0 Hz, 2H), 6.30 (d, J = 2.8 Hz, 1H), 5.63 (d, J = 2.5 Hz, 1H), 4.47□4.43 (m, 1H), 4.01 (dd, J = 9.0, 5.7 Hz, 1H), 3.11–3.03 (m, 1H), 2.69 (t, J = 7.5 Hz, 2H), 2.08–2.01 (m, 1H), 1.90–1.82 (m, 1H); ^{13}C NMR (125 MHz, DMSO): δ 170.33, 141.32, 138.74, 133.38(2C), 128.15(2C), 125.92, 121.65, 70.71, 37.74, 34.81, 31.92; HR-ESI-MS calcd for $C_{13}H_{15}O_2$ $[M + H]^+$ 203.2490, found 203.2493; IR (KBr) ν_{max} 1932, 1760, 1647, 1533, 1469, 1254, 1120, 1013, 931 cm^{-1}; *S*-**7**: [α]20 D – 37.9 (*c* 0.1, CH_2Cl_2); *R*-**8**: [α]20 D + 28.3 (*c* 0.1, CH_2Cl_2).

2-(4-methylene-5-oxotetrahydrofuran-3-yl)ethyl (4-bromophenyl)carbamate (9)

p-Bromophenyl carbamate (207 mg, 1.05 mmol) and Et_3N (106 mg, 1.05 mmol) were added to the

solution of **6** (142 mg, 1.0 mmol) in CH_2Cl_2 (10 ml) at 0 ºC. The reaction mixture was stirred for 2 h at rt, diluted with water, The aq layer was extracted with CH_2Cl_2 (3 × 10 mL) and the combined organic extracts dried by Na_2SO_4, concentrated under reduced pressure and purified by column chromatography to give **9** (275 mg, 81%) as yellow powder. The crystals of *S*-**9** and *R*-**9** were acquired from CH_2Cl_2 solution, which further analyzed by Cu Kα radiation to give their absolute configuration as drawn (**Scheme 1**).

^{1}H NMR (500 MHz, $CDCl_3$): δ 7.41 (d, J = 8.7 Hz, 2H), 7.29 (d, J = 8.2 Hz, 2H), 6.31 (d, J = 2.7 Hz, 1H), 5.67 (d, J = 2.3 Hz, 1H), 4.52 (t, J = 8.6 Hz, 1H), 4.32□4.22 (m, 2H), 4.07 (dd, J = 9.1, 5.6 Hz, 1H), 3.21 (ddd, J = 8.1, 5.5, 2.6 Hz, 1H), 2.14–2.00 (m, 1H), 1.92 (ddd, J = 14.2, 7.9, 5.7 Hz, 1H); ^{13}C NMR (125 MHz, $CDCl_3$): δ 170.63, 153.12, 137.79, 136.88, 132.1(2C), 122.68(2C), 120.44, 116.34, 71.03, 62.45, 36.41, 32.92; HR-ESI-MS calcd for $C_{14}H_{14}BrNO_4$ $[M + H]^+$ 340.1693, found 340.1701; mp 98–105 ºC; IR (KBr) ν_{max} 3340, 2956, 1772, 1731, 1656, 1532, 1491, 1400, 1225, 1160, 1096, 898, 764, 670 cm^{-1}; *S*-**9**: [α]20 D – 32.2 (*c* 0.1, CH_2Cl_2); *R*-**9**: [α]20 D + 43.6 (*c* 0.1, CH_2Cl_2).

Crystallographic data of *S*-**9**: $C_{14}H_{14}BrNO_4$, CH_2Cl_2, M = 340.17, Monoclinic, space group $P2$ (1), a = 6.2427 (12) Å, α = 90°; b = 19.473 (4) Å, β = 104.370(3)°; c = 11.986 (2) Å, γ = 90°; V = 1411.5 (5) Å^3, Z = 4, ρ_{calcd} = 1.601 mg/m^3, crystal size 0.30 × 0.06 × 0.04 mm^3. Cu Kα (λ = 0.71073 Å), F (000) = 688, T = 140 (2) K. The final R values were R_1 = 0.0353, and wR_2 = 0.0835, for 13762 observed reflections [I > 2σ (I)]. The absolute structure parameter was 0.018 (6).

Crystallographic data of *R*-**9**: $C_{14}H_{14}BrNO_4$, CH_2Cl_2, M = 340.17, Monoclinic, space group $P2$ (1), a = 6.2368 (15) Å, α = 90°; b = 19.469 (5) Å, β = 104.381(4)°; c = 11.972 (3) Å, γ = 90°; V = 1408.2 (6) Å^3, Z = 4, ρ_{calcd} = 1.605 mg/m^3, crystal size 0.30 × 0.06 × 0.04 mm^3. Cu Kα (λ = 0.71073 Å), F (000) = 688, T = 140 (2) K. The final R values were R_1 = 0.0418, and wR_2 = 0.0802, for 13779 observed reflections [I > 2σ (I)]. The absolute structure parameter was 0.016 (8).

Crystallographic data for *S*-**9** and *R*-**9** have been deposited at the Cambridge Crystallographic Data Centre (deposition NO. CCDC 934198 and 934199). Copies of the data could be obtained free of charge on application to the Director, CCDC, 12 Union Road, Cambridge CB2 1EZ, UK (fax: +44 1223 336033 or e-mail: data_request@ ccdc.cam.ac.uk).

5 Spectroscopic analysis of compounds 2 and 3

The structure of compound **2** was established by combinative analysis of MS and NMR spectroscopy. The ^{1}H and ^{13}C NMR spectra of **2** revealed the presence of a 2,6-dimethylphenyl unit and a typical α-methyl-γ-lactone unit (**Table S5**). The ^{1}H–^{1}H COSY experiment further established the H_2-9/H_2-8/H-7/H-11/H_3-13 and H-7/H_2-6 spin system (**Fig. S5**). In the HMBC spectrum, the correlations from H_2-9 to C-4/10 and from H_2-6 to C-12 and C-13 further connected the 2,6-dimethylphenyl and α-methyl-γ-lactone unit by two methylenes (**Fig. S5**). The relative configuration of **2** was established by a NOESY experiment using deuterated pyridine. The NOESY correlations of H-7 with H-6b and H_3-13 suggested their α orientation, while those of H-11 with H-6a suggested their β orientation (**Fig. S6**). Thus, the absolute structure of **2** was determined as 7*S*,11*S*.

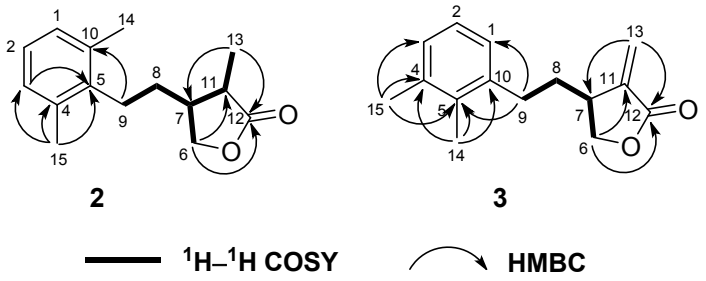

Fig. S5 Key ^{1}H–^{1}H COSY and HMBC correlations of compounds **2** and **3**.

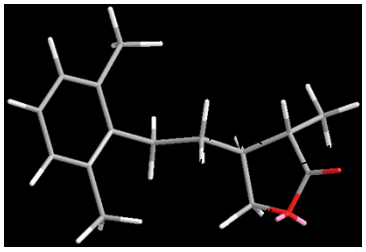

Fig. S6 Key NOESY correlations of compound **2**.

Table S5 ^{1}H and ^{13}C NMR spectroscopic data for compounds **2** and **3**

No.	**2**			**3**	
	δ_C[a]	δ_H (mult, *J* in Hz)[b]	δ_H (mult, *J* in Hz)[c]	δ_C[d]	δ_H (mult, *J* in Hz)[e]
1	128.4 d	7.01 m (overlap)	7.17 m (overlap)	127.0 d	6.97 m
2	126.1 d	7.01 m (overlap)	7.17 m (overlap)	125.8 d	7.04 m (overlap)
3	128.4 d	7.01 m (overlap)	7.17 m (overlap)	128.5 d	7.04 m (overlap)
4	135.6 s			136.5 s	
5	137.8 s			134.5 s	
6a	71.4 t	4.48 dd (8.0, 7.5)	4.49 dd (8.0, 7.5)	71.2 t	4.49 dd (8.4, 8.4)
6b		3.87 dd (9.0, 9.0)	3.88 dd (9.0, 9.0)		4.03 dd (8.4, 5.6)
7	40.5 d	2.26 m (overlap)	2.34 m	38.8 d	3.11 m
8a	31.4 t	1.80 m	1.69 m	34.8 t	1.96 m
8b		1.55 m	1.49 m		1.78 m
9	27.3 t	2.65 m	2.61 m	31.0 t	2.70 dd (7.6, 7.6)
10	135.6 s			139.8 s	
11	44.3 d	2.26 m (overlap)	2.19 m	137.9 s	
12	179.5 s			172.0 s	
13a	14.2 q	1.31 d (6.0)	1.33 d (7.0)	122.2 t	6.34 d (2.8)
13b					5.63 d (2.8)
14	19.8 q	2.32 s	2.34 s	15.2 q	2.20 s
15	19.8 q	2.32 s	2.34 s	20.8 q	2.29 s

[a] Data were recorded in $CDCl_3$ at 125 MHz for ^{13}C NMR;

[b] Data were recorded in $CDCl_3$ at 500 MHz for ^{1}H NMR;

[c] Data were recorded in C_5D_5N at 500 MHz for ^{1}H NMR;

[d] Data were recorded in $CDCl_3$ at 100 MHz for ^{13}C NMR;

[e] Data were recorded in $CDCl_3$ at 400 MHz for ^{1}H NMR.

Likewise, a 2,3-dimethylphenyl unit and a typical α-methylene-γ-lactone unit were revealed by ^{1}H and ^{13}C NMR spectra of **3** (**Table S5**), which were further connected by two methylenes established by extensive analyses of ^{1}H–^{1}H COSY and HMBC spectra (**Fig. S5**). The negative Cotton effect at 218 nm in the CD spectrum of **3** determined its 7*S* configuration.

Winolide A (1)

Colorless oil; $C_{15}H_{18}O_2$; [α]20 D − 91.2 (*c* 0.1, CH_2Cl_2); UV (MeOH) λ_{max} (logε): 220 (3.15) nm; IR (KBr) ν_{max} 2952, 1765, 1661, 1489, 1405, 1267, 1165, 1115, 1013, 947 cm^{-1}; ESIMS *m/z* 253.1 $[M + Na]^+$, *m/z* 229.1 $[M - H]^-$; HR-ESI-MS *m/z* 253.1206 $[M + Na]^+$ (calcd for $C_{15}H_{18}O_2Na$, 253.1204); ^{1}H and ^{13}C NMR data, see **Table 1**.

Winolide B (2)

Colorless oil; $C_{15}H_{20}O_2$; [α]20 D − 29.3 (*c* 0.05, MeOH); UV (MeOH) λ_{max} (logε): 220 (2.69) nm; IR (KBr) ν_{max} 2929, 1774, 1589, 1464, 1384, 1240, 1187, 1164, 1099, 1016 cm^{-1}; ESIMS *m/z* 255.1 $[M + Na]^+$, *m/z* 231.1 $[M - H]^-$; HR-ESI-MS *m/z* 255.1365 $[M + Na]^+$ (calcd for $C_{15}H_{20}O_2Na$, 255.1361); ^{1}H and ^{13}C NMR data, see **Table S5**.

Winolide C (3)

Colorless oil; $C_{15}H_{18}O_2$; [α]20 D − 16.6 (*c* 0.05, CH_2Cl_2); UV (MeOH) λ_{max} (logε): 220 (2.56) nm; IR (KBr) ν_{max} 2925, 2857, 1763, 1628, 1547, 1462, 1379, 1267, 1119, 1013 cm^{-1}; ESIMS *m/z* 253.1 $[M + Na]^+$, *m/z* 229.1 $[M - H]^-$; HR-ESI-MS *m/z* 253.1204 $[M + Na]^+$ (calcd for $C_{15}H_{18}O_2Na$, 253.1204); ^{1}H and ^{13}C NMR data, see **Table S5**.

6 Bioassay for compounds 1–3

The NO inhibitory assay was conducted according to procedures previously described. Briefly, RAW264.7 macrophages grown on 100 mm culture dishes were harvested and seeded in 96-well plates at 2 × 10_5 cells/well for NO production. The plates were pretreated with various concentrations of samples (20, 5, 0.5, and 0.1μM) for 30 min and then incubated for 24 h with or without 1 μg/mL of LPS. Aminoguanidine (Sigma-Aldrich, purity ≥ 98.0%) was used as a positive control (IC_{50} = 0.37 μM). The nitrite concentration in the culture supernatant was measured by the Griess reaction. Cell viability was measured using MTT [3-(4,5-dimethylthiazol-2-yl)-2,5-diphenyltetrazolium bromide] assays (Sigma-Aldrich).

7 NMR spectra for compounds 1–9

Fig. S7 ^{1}H NMR spectrum ($CDCl_3$, 400 MHz) of compound **1**
Fig. S8 ^{13}C NMR spectrum ($CDCl_3$, 100 MHz) of compound **1**
Fig. S9 DEPT spectrum ($CDCl_3$, 100 MHz) of compound **1**
Fig. S10 HSQC spectrum ($CDCl_3$, 400 MHz) of compound **1**
Fig. S11 ^{1}H–^{1}H COSY spectrum ($CDCl_3$, 400 MHz) of compound **1**
Fig. S12 HMBC spectrum ($CDCl_3$, 400 MHz) of compound **1**
Fig. S13 ^{1}H NMR spectrum ($CDCl_3$, 500 MHz) of compound **2**
Fig. S14 ^{13}C NMR spectrum ($CDCl_3$, 125 MHz) of compound **2**
Fig. S15 DEPT spectrum ($CDCl_3$, 125 MHz) of compound **2**
Fig. S16 HSQC spectrum ($CDCl_3$, 500 MHz) of compound **2**
Fig. S17 ^{1}H–^{1}H COSY spectrum ($CDCl_3$, 500 MHz) of compound **2**
Fig. S18 HMBC spectrum ($CDCl_3$, 500 MHz) of compound **2**
Fig. S19 ^{1}H NMR spectrum (C_5D_5N, 500 MHz) of compound **2**
Fig. S20 NOESY spectrum (C_5D_5N, 500 MHz) of compound **2**
Fig. S21 ^{1}H NMR spectrum ($CDCl_3$, 400 MHz) of compound **3**
Fig. S22 ^{13}C NMR spectrum ($CDCl_3$, 100 MHz) of compound **3**
Fig. S23 HSQC spectrum ($CDCl_3$, 400 MHz) of compound **3**
Fig. S24 ^{1}H–^{1}H COSY spectrum ($CDCl_3$, 400 MHz) of compound **3**
Fig. S25 HMBC spectrum ($CDCl_3$, 400 MHz) of compound **3**
Fig. S26 ^{1}H NMR spectrum ($CDCl_3$, 500 MHz) of compound **4**
Fig. S27 ^{13}C NMR spectrum ($CDCl_3$, 125 MHz) of compound **4**
Fig. S28 ^{1}H NMR spectrum ($CDCl_3$, 600 MHz) of compound **5**
Fig. S29 ^{13}C NMR spectrum ($CDCl_3$, 150 MHz) of compound **5**
Fig. S30 ^{1}H NMR spectrum ($CDCl_3$, 500 MHz) of compound **6**
Fig. S31 ^{13}C NMR spectrum ($CDCl_3$, 125 MHz) of compound **6**
Fig. S32 ^{1}H NMR spectrum ($CDCl_3$, 500 MHz) of compound **7**
Fig. S33 ^{13}C NMR spectrum ($CDCl_3$, 125 MHz) of compound **7**
Fig. S34 ^{1}H NMR spectrum ($CDCl_3$, 500 MHz) of compound **8**
Fig. S35 ^{13}C NMR spectrum (DMSO-d_6, 125 MHz) of compound **8**
Fig. S36 ^{1}H NMR spectrum ($CDCl_3$, 500 MHz) of compound **9**
Fig. S37 ^{13}C NMR spectrum ($CDCl_3$, 125 MHz) of compound **9**

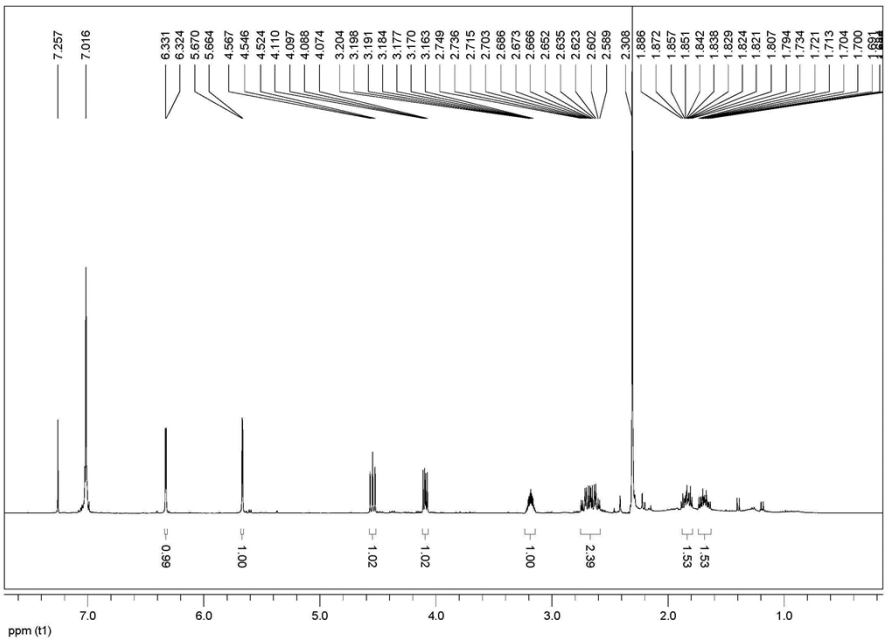

Fig. S7 ^{1}H NMR spectrum ($CDCl_3$, 400 MHz) of compound **1**

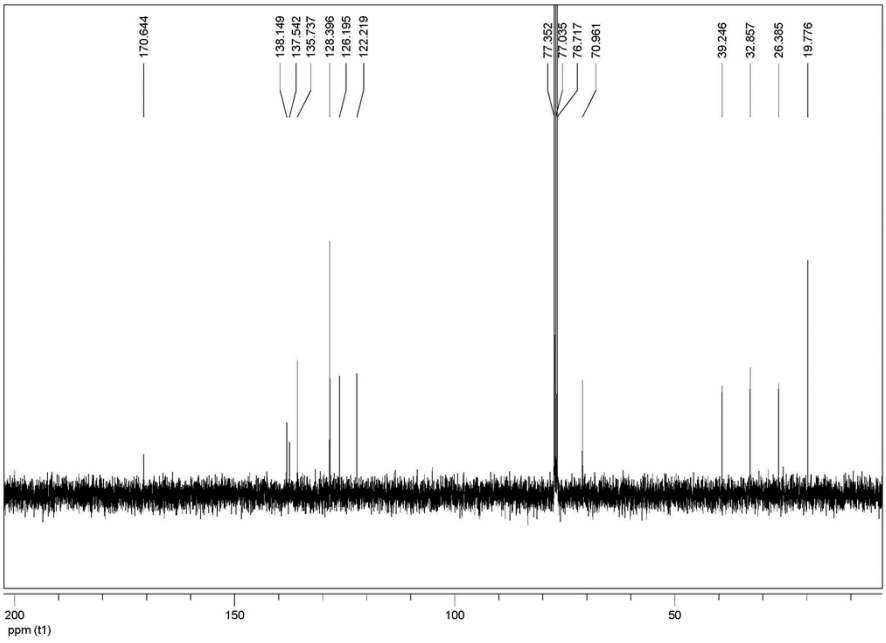

Fig. S8 ^{13}C NMR spectrum ($CDCl_3$, 100 MHz) of compound **1**

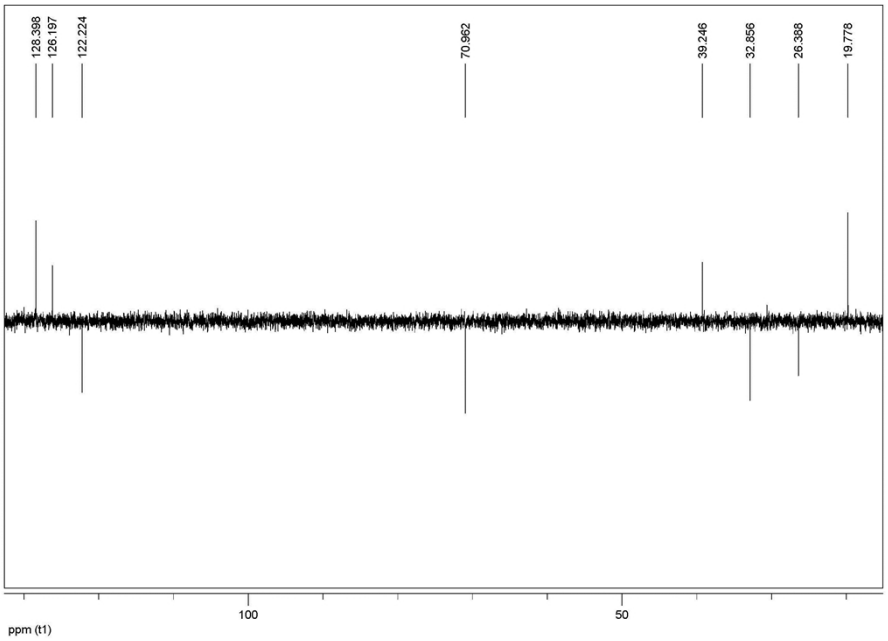

Fig. S9 DEPT spectrum ($CDCl_3$, 100 MHz) of compound **1**

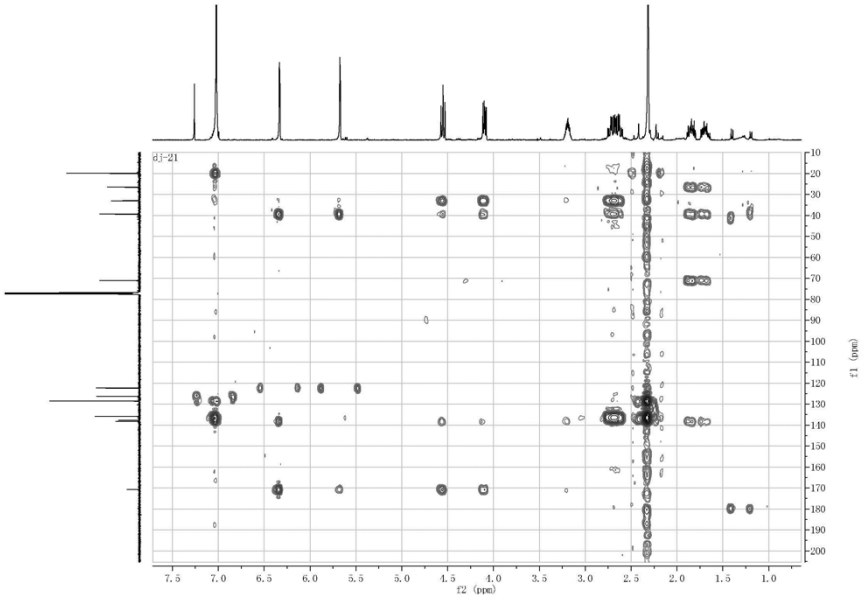

Fig. S10 HSQC spectrum ($CDCl_3$, 400 MHz) of compound **1**

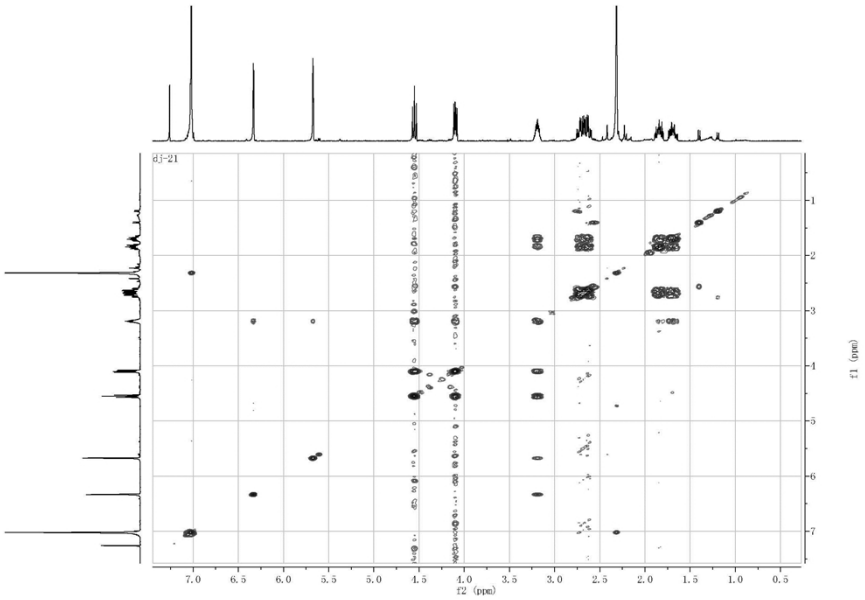

Fig. S11 $^{1}H-^{1}H$ COSY spectrum ($CDCl_3$, 400 MHz) of compound **1**

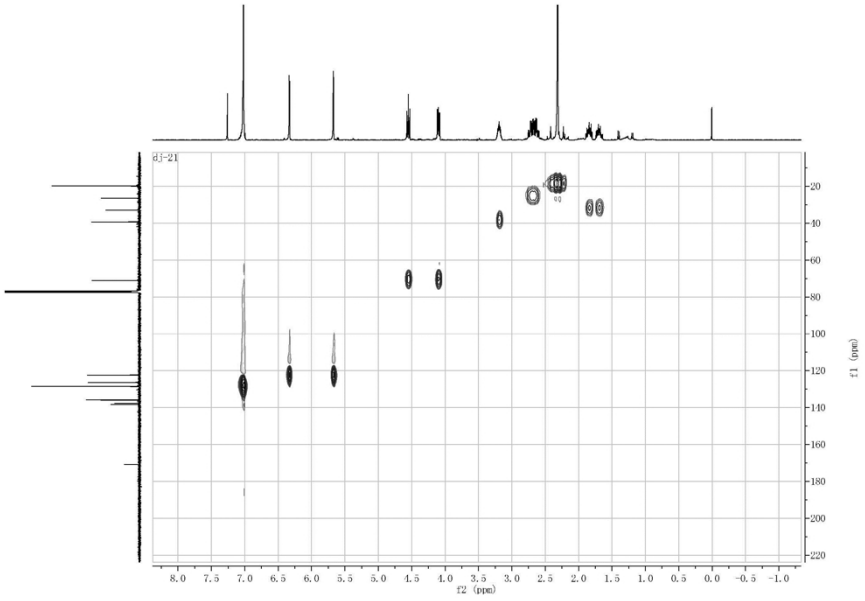

Fig. S12 HMBC spectrum ($CDCl_3$, 400 MHz) of compound **1**

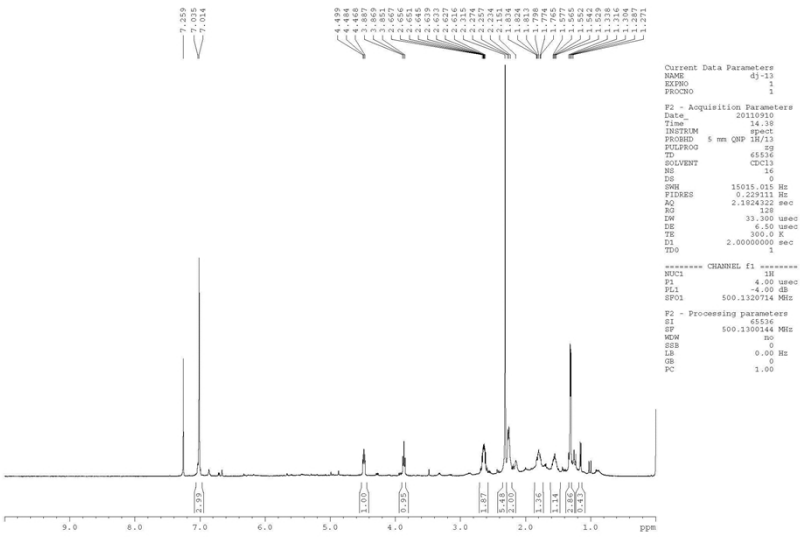

Fig. S13 ^{1}H NMR spectrum ($CDCl_3$, 500 MHz) of compound **2**

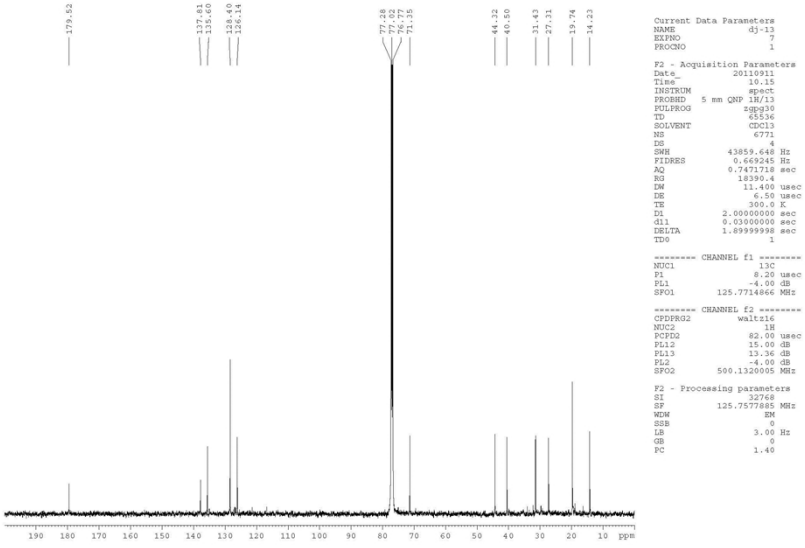

Fig. S14 ^{13}C NMR spectrum ($CDCl_3$, 125 MHz) of compound **2**

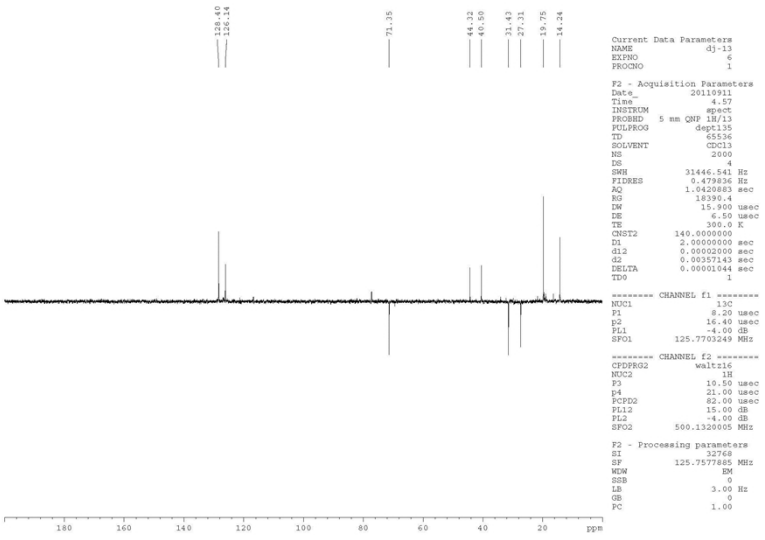

Fig. S15 DEPT spectrum ($CDCl_3$, 125 MHz) of compound **2**

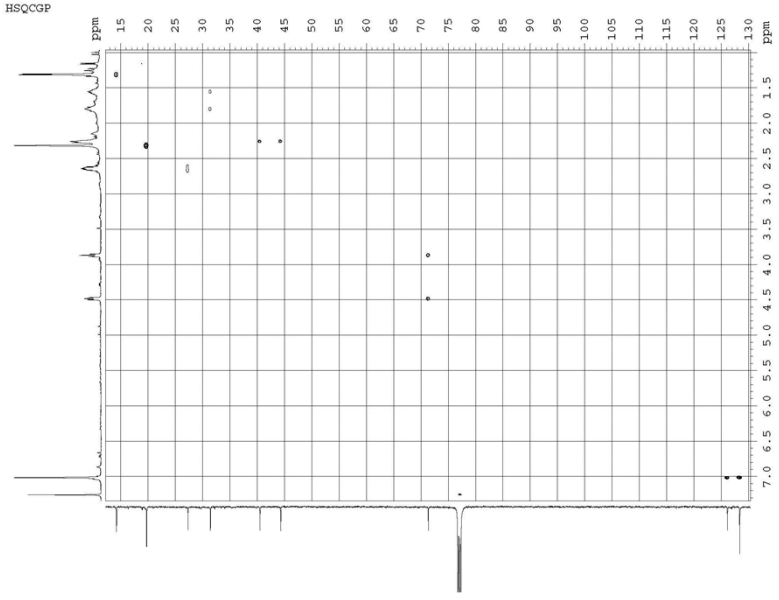

Fig. S16 HSQC spectrum ($CDCl_3$, 500 MHz) of compound **2**

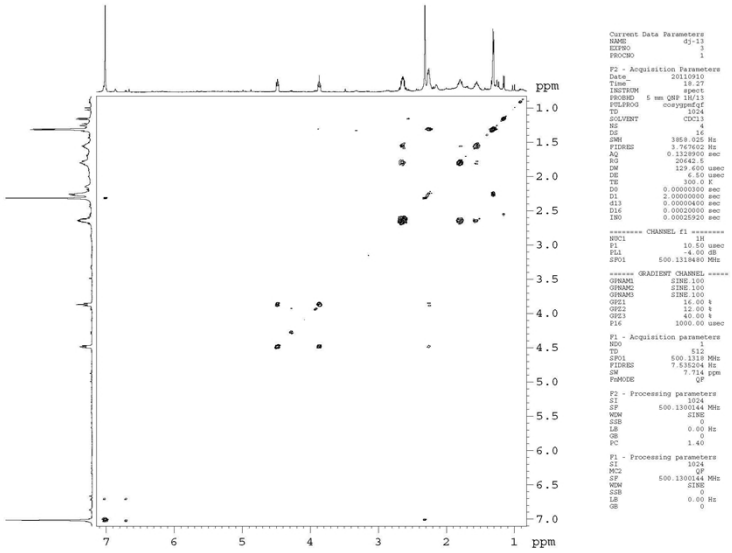

Fig. S17 $^{1}H-^{1}H$ COSY spectrum ($CDCl_3$, 500 MHz) of compound **2**

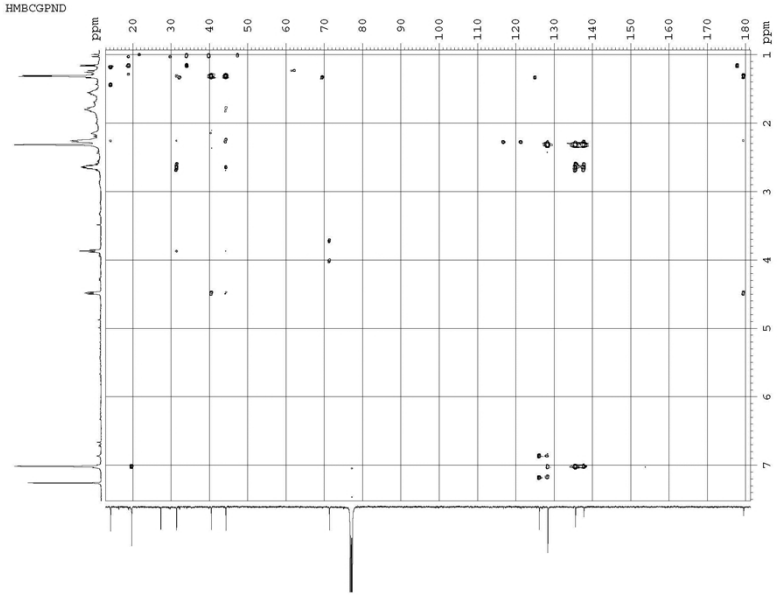

Fig. S18 HMBC spectrum ($CDCl_3$, 500 MHz) of compound **2**

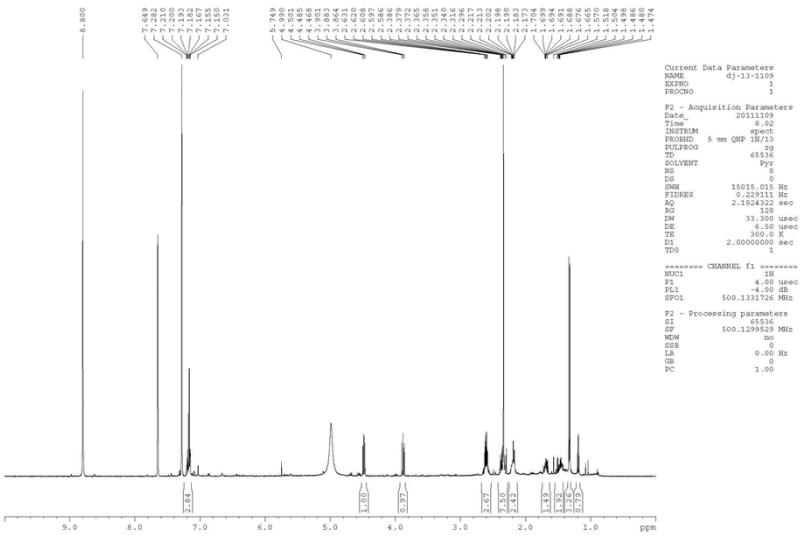

Fig. S19 ^{1}H NMR spectrum (C_5D_5N, 500 MHz) of compound **2**

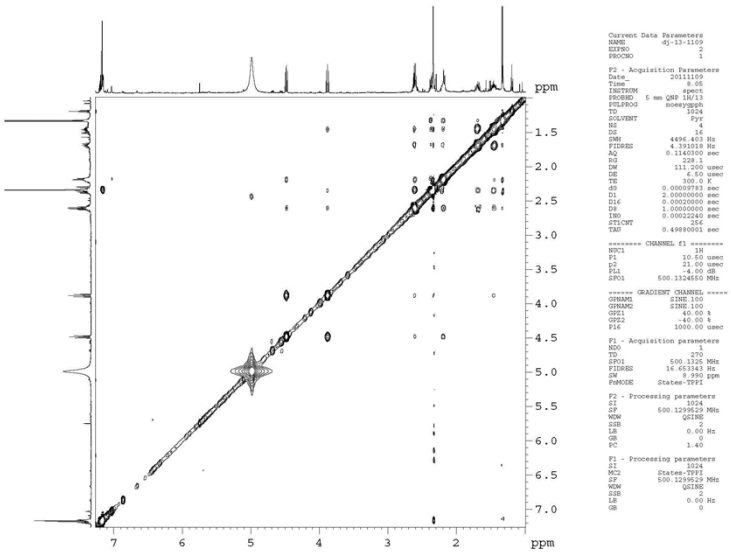

Fig. S20 NOESY spectrum (C_5D_5N, 500 MHz) of compound **2**

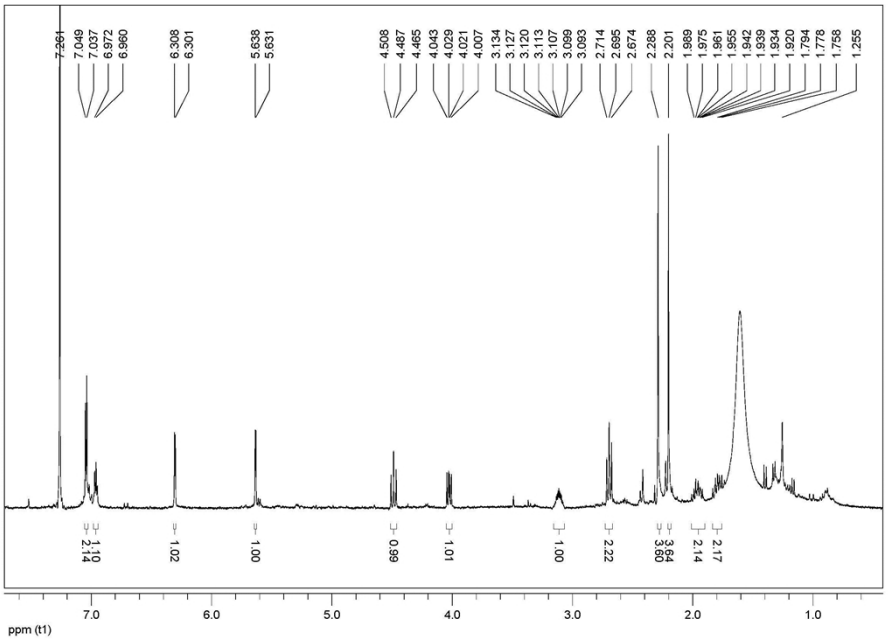

Fig. S21 ^{1}H NMR spectrum ($CDCl_3$, 400 MHz) of compound **3**

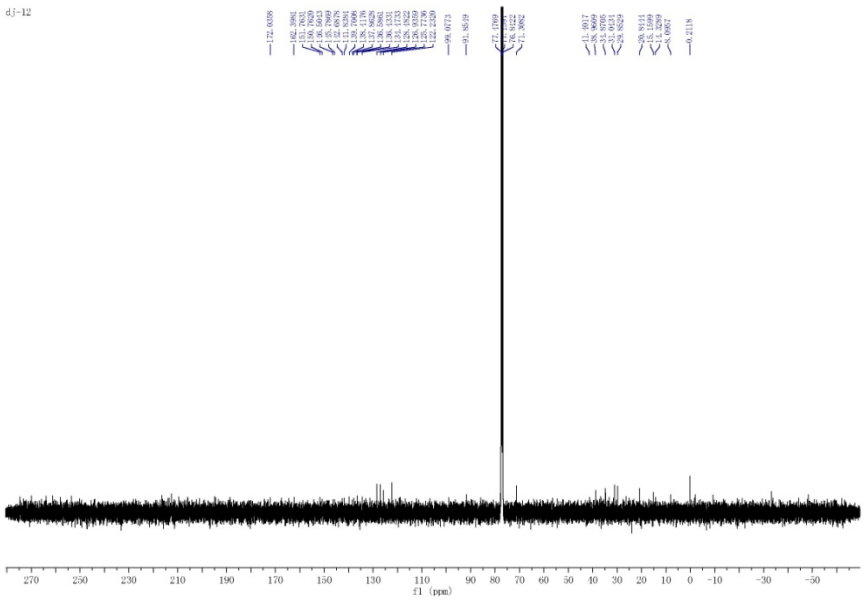

Fig. S22 ^{13}C NMR spectrum ($CDCl_3$, 100 MHz) of compound **3**

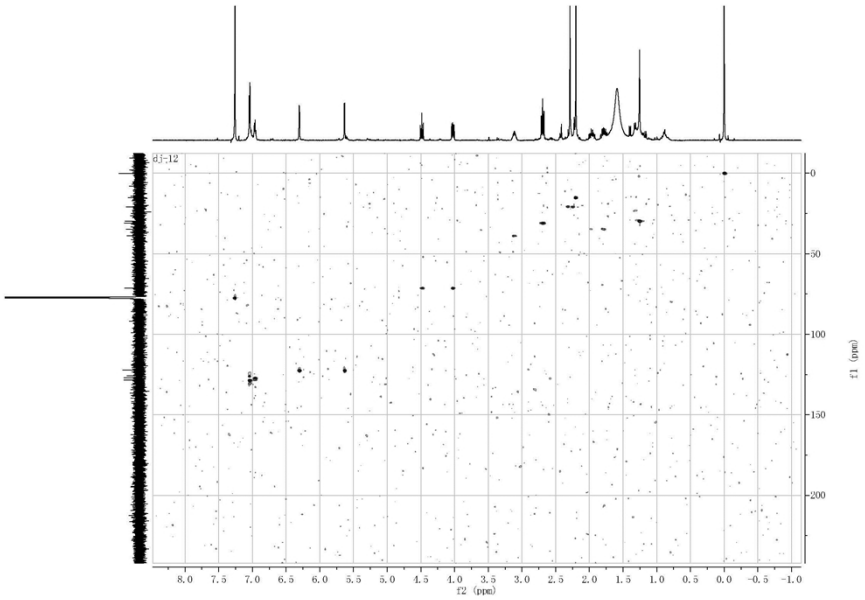

Fig. S23 HSQC spectrum ($CDCl_3$, 400 MHz) of compound **3**

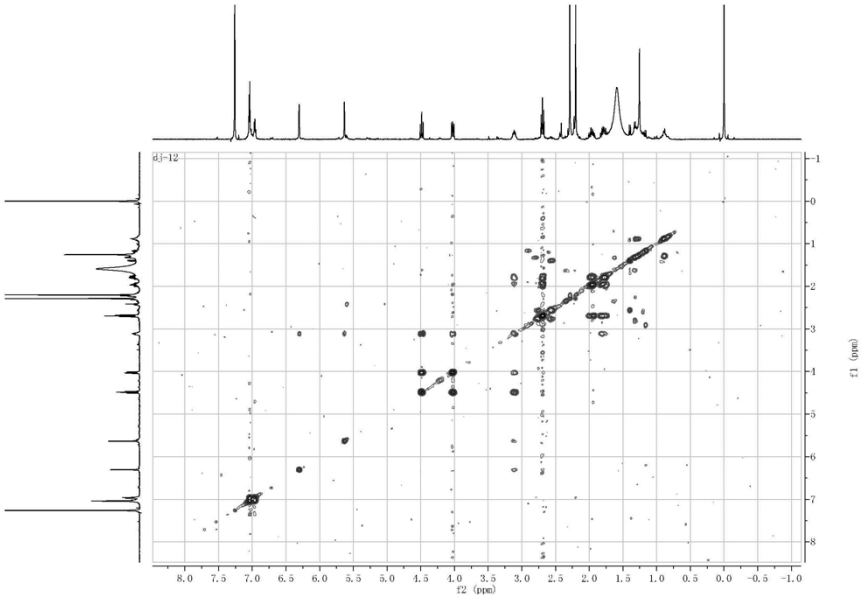

Fig. S24 ^1H–^1H COSY spectrum ($CDCl_3$, 400 MHz) of compound **3**

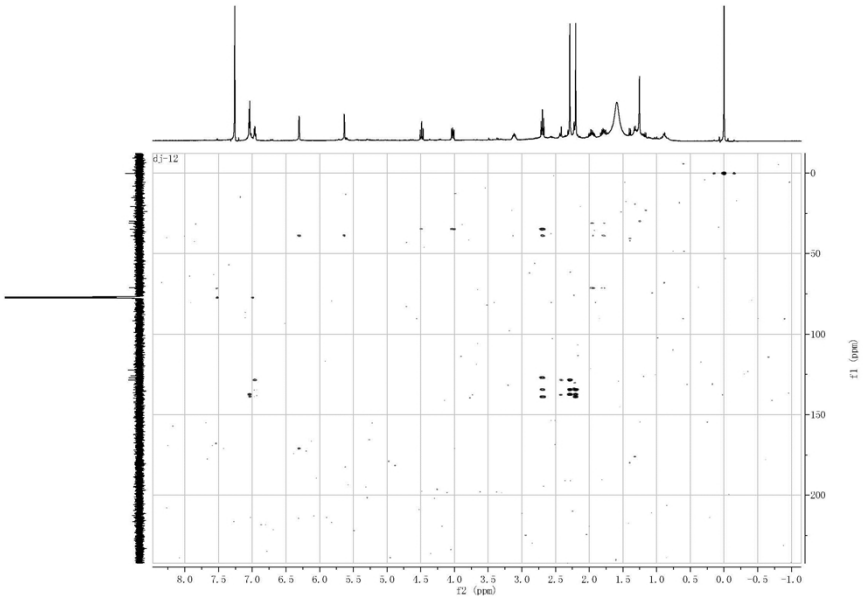

Fig. S25 HMBC spectrum ($CDCl_3$, 400 MHz) of compound **3**

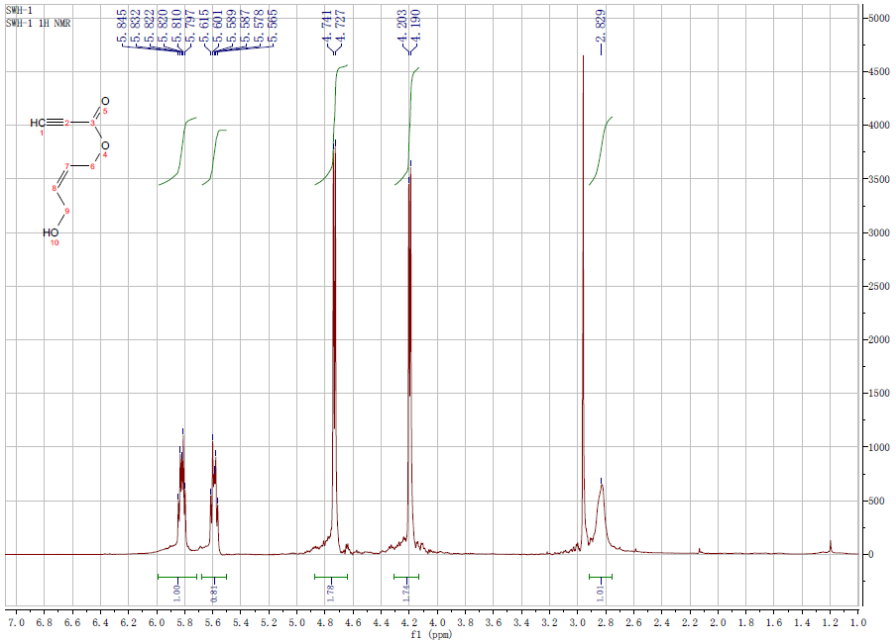

Fig. S26 ^1H NMR spectrum ($CDCl_3$, 500 MHz) of compound **4**

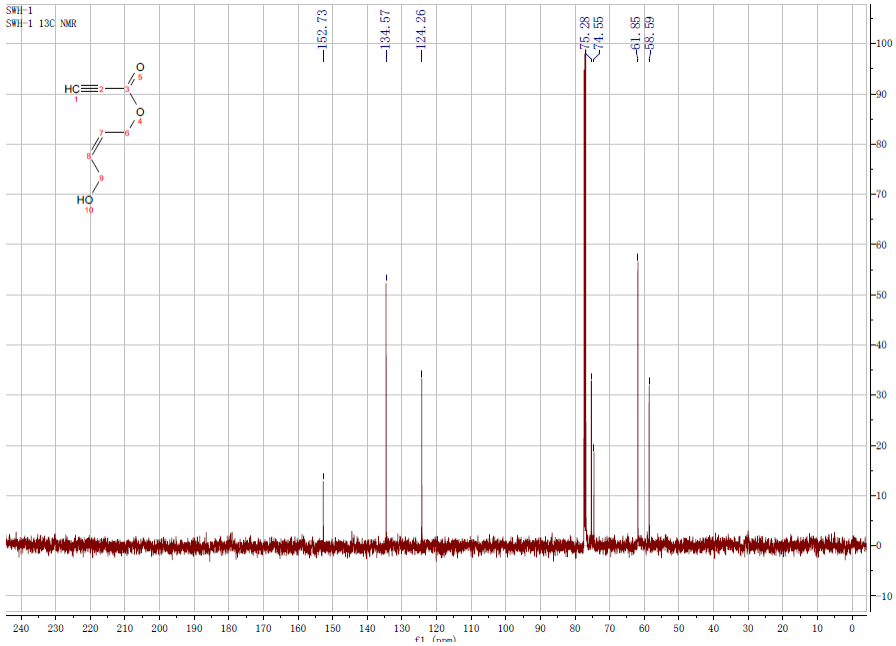

Fig. S27 ^{13}C NMR spectrum ($CDCl_3$, 125 MHz) of compound **4**

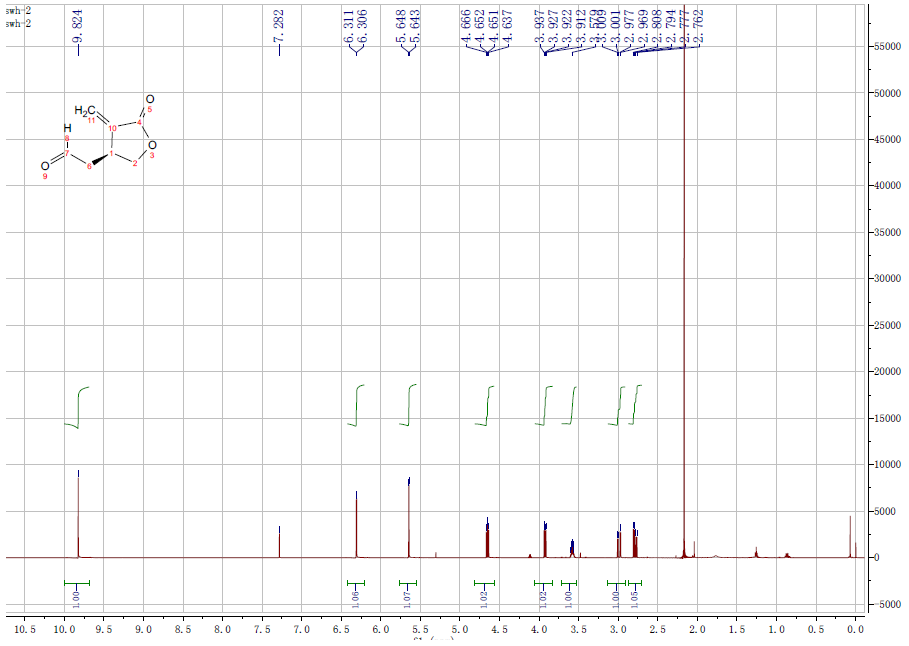

Fig. S28 ^{1}H NMR spectrum ($CDCl_3$, 600 MHz) of compound **5**

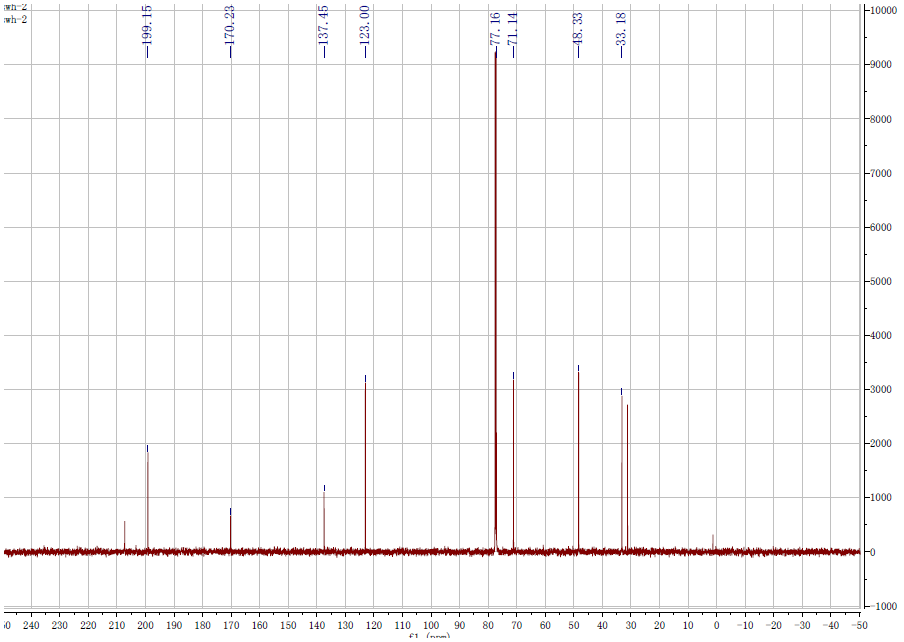

Fig. S29 ^{13}C NMR spectrum ($CDCl_3$, 150 MHz) of compound **5**

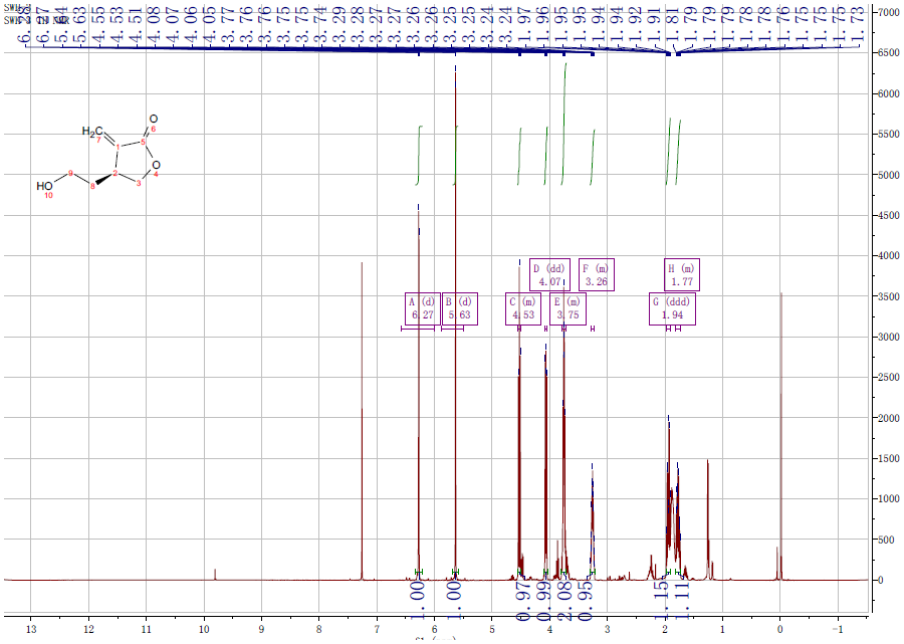

Fig. S30 ^{1}H NMR spectrum ($CDCl_3$, 500 MHz) of compound **6**

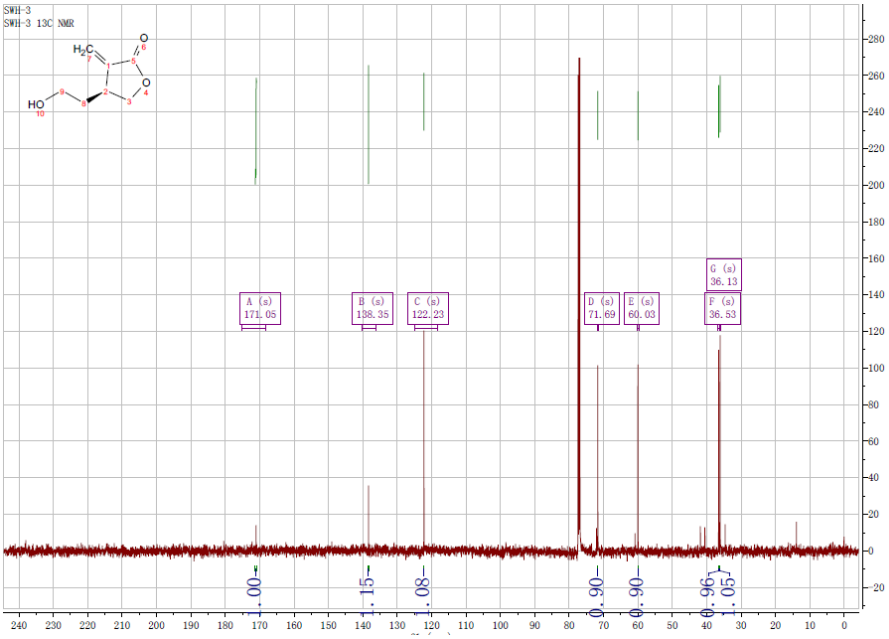

Fig. S31 ^{13}C NMR spectrum ($CDCl_3$, 125 MHz) of compound **6**

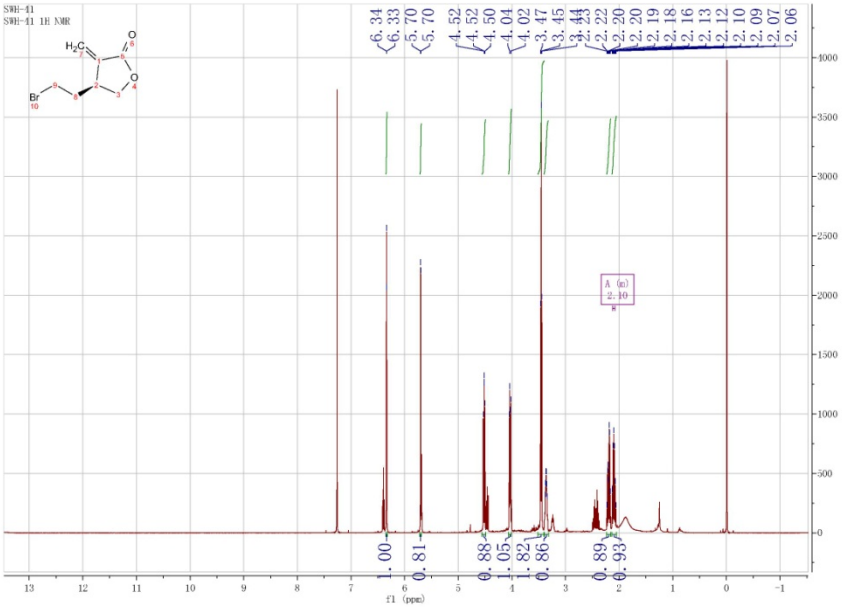

Fig. S32 ^{1}H NMR spectrum ($CDCl_3$, 500 MHz) of compound **7**

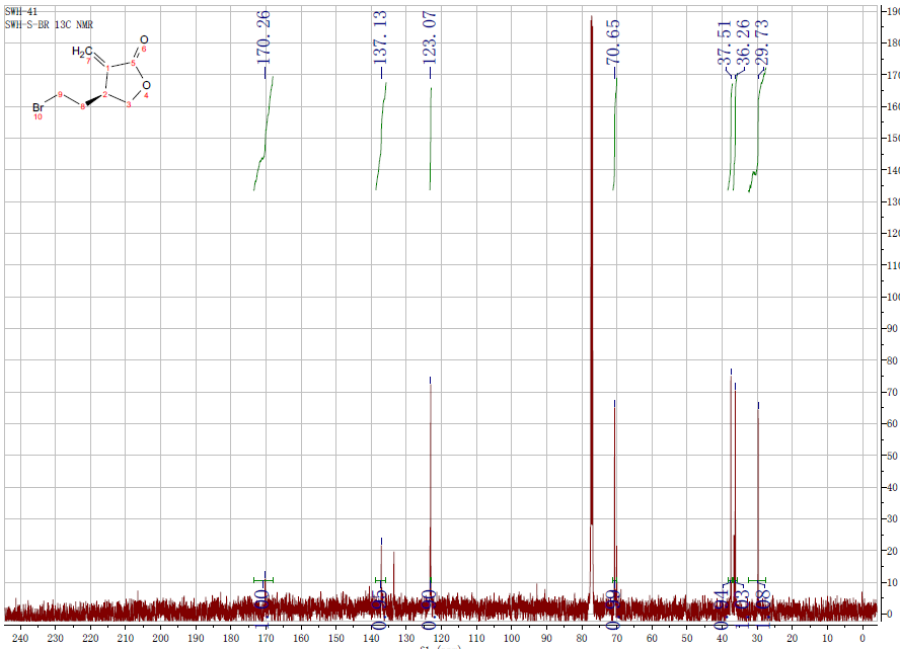

Fig. S33 ^{13}C NMR spectrum ($CDCl_3$, 125 MHz) of compound **7**

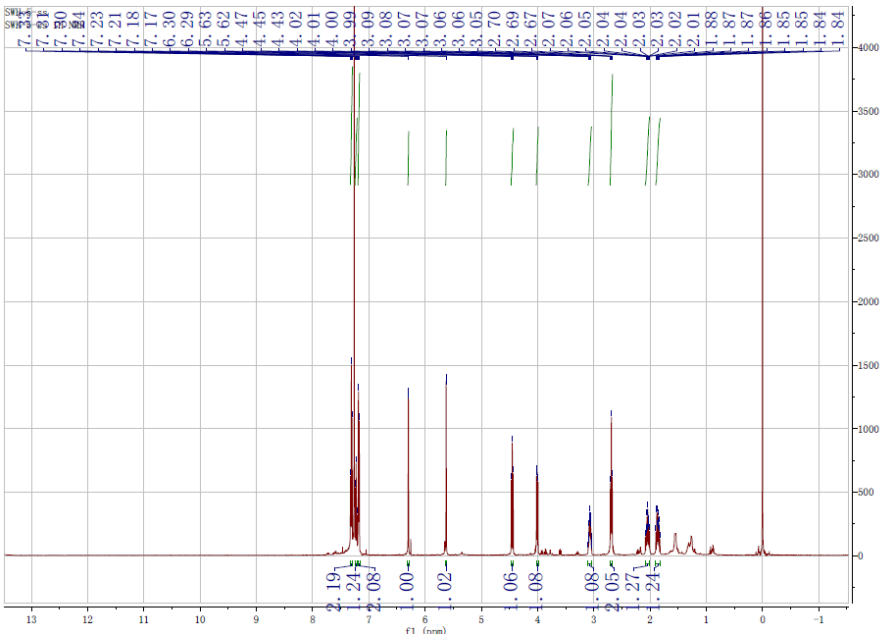

Fig. S34 ^{1}H NMR spectrum ($CDCl_3$, 500 MHz) of compound **8**

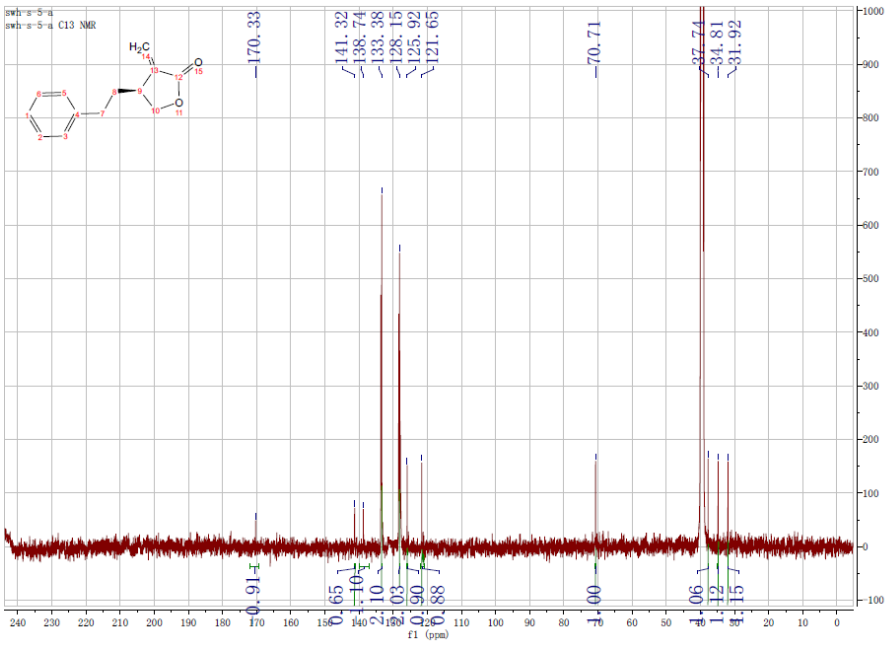

Fig. S35 ^{13}C NMR spectrum (DMSO-d_6, 125 MHz) of compound **8**

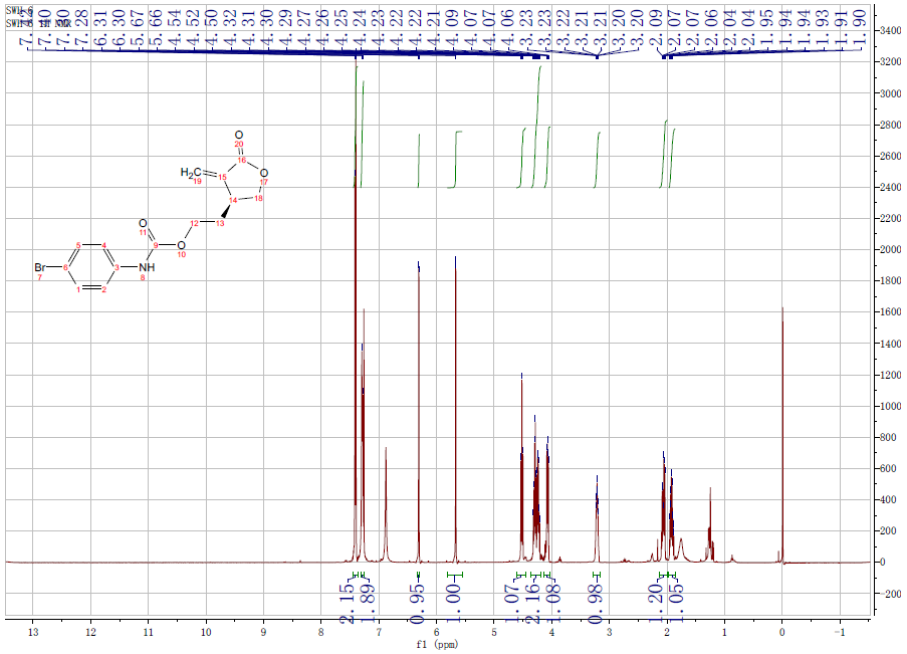

Fig. S36 ^{1}H NMR spectrum ($CDCl_3$, 500 MHz) of compound **9**

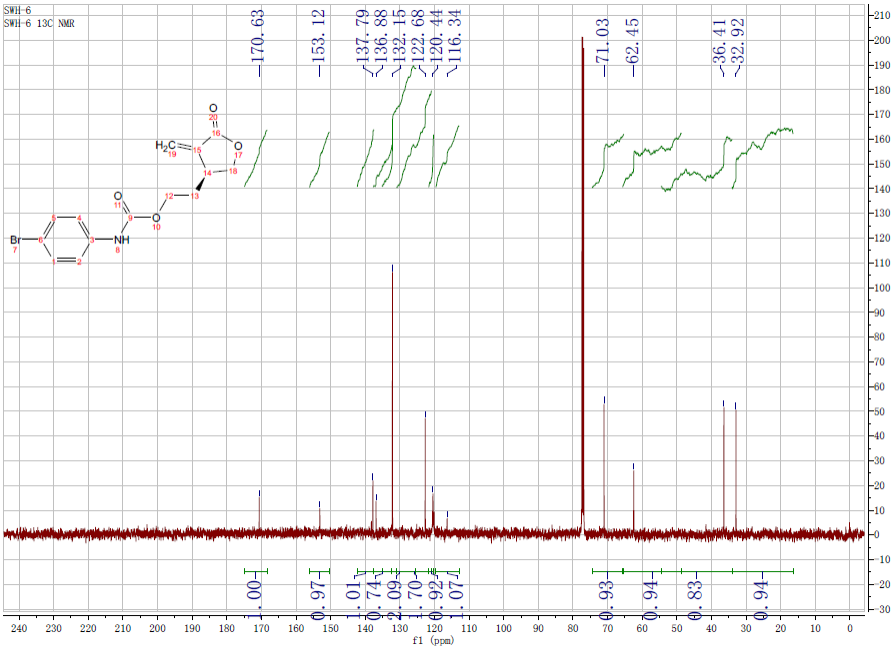

Fig. S37 ^{13}C NMR spectrum ($CDCl_3$, 125 MHz) of compound **9**